

RESEARCH ARTICLE

10.1029/2018JC014502

Special Section:

Recent Progresses in Oceanography and Air-Sea Interactions in Southeast Asian Archipelago

This article is a companion to Pujiana et al. (2019), <https://doi.org/10.1029/2018JC014574>.**Key Points:**

- This 13.3-year record of Makassar Strait throughflow displays fluctuations over a broad range of time scales: intraseasonal to interannual
- Stronger southward transport and shallower velocity maximum occur during boreal summer and during La Niña, than occur in winter and El Niño
- Makassar Strait throughflow decreased during the 2015 El Niño to ~10 Sv, increasing to ~20 Sv during the 2017 La Niña






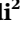
Correspondence to:A. L. Gordon,
agordon@ldeo.columbia.edu**Citation:**Gordon, A. L., Napitu, A., Huber, B. A., Gruenborg, L. K., Pujiana, K., Agustidi, T., et al. (2019). Makassar Strait throughflow seasonal and interannual variability: An overview. *Journal of Geophysical Research: Oceans*, 124, 3724–3736. <https://doi.org/10.1029/2018JC014502>

Received 23 AUG 2018

Accepted 5 FEB 2019

Accepted article online 30 APR 2019

Published online 13 JUN 2019

Makassar Strait Throughflow Seasonal and Interannual Variability: An OverviewArnold L. Gordon¹ , Asmi Napitu^{1,2} , Bruce A. Huber¹ , Laura K. Gruenborg¹ , Kandaga Pujiana^{1,3,4} , Teguh Agustidi² , Anastasia Kuswardani², Nurman Mbay², and Agus Setiawan²¹Lamont-Doherty Earth Observatory, Columbia University, Palisades, NY, USA, ²Ministry of Marine Affairs and Fisheries, Jakarta, Indonesia, ³Bandung Institute of Technology, Bandung, Indonesia, ⁴NOAA Pacific Marine Environmental Laboratory, Seattle, WA, USA

Abstract The Makassar Strait throughflow of ~12–13 Sv, representing ~77% of the total Indonesian Throughflow, displays fluctuations over a broad range of time scales, from intraseasonal to seasonal (monsoonal) and interannual scales. We now have 13.3 years of Makassar throughflow observations: November 1996 to early July 1998; January 2004 to August 2011; and August 2013 to August 2017. Strong southward transport is evident during boreal summer, modulated by an ENSO interannual signal, with weaker southward flow and a deeper subsurface velocity maximum during El Niño; stronger southward flow with a shallower velocity maximum during La Niña. Accordingly, the southward heat flux, a product of the along-channel current and temperature profiles, is significantly larger in summer and slightly larger during La Niña. The southward flow relaxed in 2014 and more so in 2015/2016, similar though not as extreme as during the strong El Niño event of 1997. In 2017, the throughflow increased to ~20 Sv. Since 2016, the deep layer, 300- to 760-m southward transport increases, almost doubling to ~7.5 Sv. From mid-2016 into early 2017, the transports above 300 m and below 300 m are about equal, whereas previously, the ratio was about 2.7:1. Near zero or northward flow occurs in the upper 100 m during boreal winter, albeit with interannual variability. Particularly strong winter reversals were observed in 2014/2015 and 2016/2017, the latter being the strongest winter reversal revealed in the entire Makassar time series.

Plain Language Summary Pacific water flows into the Indian Ocean within the passages and basins of the Indonesian Seas: the Indonesian Throughflow (ITF), driven by the pressure gradient between the Pacific and Indian Oceans. The ITF affects heat and freshwater inventories of the Pacific and Indian Oceans. The primary inflow path of Pacific water into the Indonesian seas is the Makassar Strait, channeling $12.5 \times 10^6 \text{ m}^3/\text{s}$, about 77% of the total ITF. During the 21 years, November 1996 to August 2017, we have recorded 13.3 years of Makassar throughflow, exposing a broad range of spatial and temporal scale patterns. The Makassar Strait annual cycle transport ranges from about 7 to $16 \times 10^6 \text{ m}^3/\text{s}$. Strong southward transport occurs during boreal summer, with weaker (stronger) southward flow and a deeper (shallower) subsurface velocity maximum during El Niño (La Niña). The throughflow relaxed in 2015 into 2016 during an El Niño. In 2017, the southward transport increased to $20 \times 10^6 \text{ m}^3/\text{s}$. The 300- to 760-m transport increased in 2016 into 2017, equaling the 0- to 300-m transport, from the more typical 30% of the 0- to 300-m transport. Near zero flow occurs in the upper ~100 m during boreal winter with particularly strong winter reversals in 2014/2015 and 2016/2017.

1. Introduction

The complex array of basins and channels of the Maritime Continent, including the Indonesian seas, forms the only tropical interocean exchange pathway of the global ocean. They provide a conduit for Pacific Ocean to reach into the Indian Ocean, forming a key component of the larger-scale ocean and climate systems. During the Arlindo Mixing program of 1993–1998, the primary pathways of the flow from the Pacific to Indian Ocean through the Indonesian seas were identified (Gordon & Fine, 1996; Ilahude & Gordon, 1996; Figure 1). Makassar Strait, with a sill depth of 680 m (Gordon, Giulivi, & Ilahude, 2003; Figure 1), serves as the westernmost deep pathway of what is referred to as the Indonesian Throughflow (ITF; Sprintall et al., 2014; Wajsowicz et al., 2003). The Makassar Strait throughflow channels North Pacific water into Lombok Strait and into the Banda Sea via the Flores Sea. The Makassar Strait throughflow is joined by inflow via

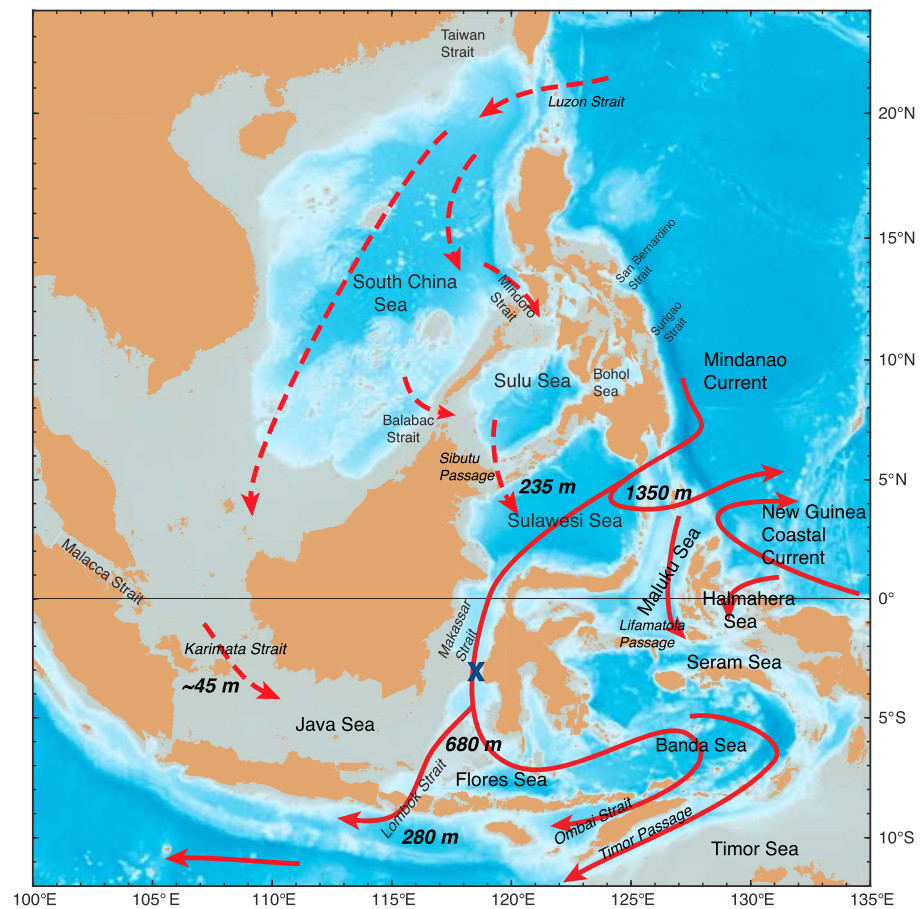


Figure 1. The pathways and sill depths of the Indonesian Throughflow within the Maritime Continent (Gordon et al., 2012). The dashed red arrows show the throughflow within the South China Sea. Modified from Gordon et al. (2012). The X symbol in Makassar Strait marks the position of the current measuring mooring in Labani Channel: at 2°51' S; 118°28' E and water depth of 2,137 m. The topographic sill of the Makassar throughflow is 680 m at the Dewakang Sill (Gordon, Giulivi, & Ilahude, 2003).

the eastern passages of Maluku Sea and Halmahera Sea and water drawn from the South China Sea via within Karimata Strait. The eastern pathways mainly draw water from the South Pacific, experiencing substantial diapycnal mixing driven by strong tidal dissipation (Field & Gordon, 1992, 1996; Koch-Larrouy et al., 2007, 2010), which significantly alter the thermohaline stratification profile within the Banda Sea (Ilahude & Gordon, 1996) before export to the Indian Ocean through the various passage of the Sunda Arc, primarily via the Timor Passage, Ombai Strait, and Lombok Strait (Atmadipoera et al., 2009; Hautala et al., 2001; Sprintall et al., 2014).

In late 1996, as part of the Arlindo Circulation program, two moorings were deployed in a restriction of Makassar Strait, the 45 km wide (at 50-m depth) Labani Channel (Figure 1), recording the ITF until mid-1998 (Field et al., 2000; Gordon et al., 1999; Susanto & Gordon, 2005). In 2004, the Labani Channel moorings were redeployed as part of the International Nusantara Stratification and Transport program (INSTANT) 2004–2006 program (Gordon et al., 2008, 2010) for the first time to simultaneously monitor the multiple pathways of the ITF. Upon the termination of the INSTANT program in December 2006, the Labani Channel time series was continued as the Monitoring the ITF (MITF; Gordon et al., 2012; Susanto et al., 2012), which has been maintained to the present, with the last mooring recovery and data download in August 2017 and redeployment in November 2017.

We now have 13.3 years (not counting time gaps) of Makassar throughflow time series: November 1996 to early July 1998; January 2004 to August 2011; and August 2013 to August 2017. The Makassar throughflow time series reveals that Makassar Strait throughflow averages 12 to 13 Sv, representing ~77% of the total ITF,

based on the ratio of the Makassar Strait throughflow to the other passages recorded during INSTANT 2004–2006 (Gordon et al., 2010). The time series displays temporal fluctuations over a broad range of scales, from intraseasonal, associated with Rossby and Kelvin Waves from the Sulawesi Sea and Indian Ocean, respectively (Pujiana et al., 2009, 2012, 2013), intraseasonal fluctuations induced by Madden-Julian Oscillations (MJO) passing over the Maritime Continent (Napitu, 2017; Shinoda et al., 2016), to seasonal (monsoonal) and interannual (ENSO) scales (Gordon et al., 2010, 2012; Susanto et al., 2012). As is the nature of a time series, knowledge of a phenomenon grows as the time series lengthens, capturing lower frequency oscillations as well as anomalous or extreme events, offering a window to the ITF coupling to the larger-scale ocean and climate systems, including heat and freshwater inventories within the Pacific and Indian Oceans.

We now present an overview of the characteristics of the Makassar throughflow revealed by the 13.3-year time series, with emphasis on the recent period, August 2013 to August 2017, not previously reported in the published literature.

2. The Makassar Data

2.1. Arlindo, December 1996 to July 1998

As part of the Indonesian-U.S. Arlindo program, velocity was measured at various depths within Makassar Strait, at two moorings, MAK-1 ($2^{\circ}52' \text{ S}$, $118^{\circ}27' \text{ E}$) and MAK-2 ($2^{\circ}51' \text{ S}$; $118^{\circ}38' \text{ E}$), at a separation of 19.4 km, deployed within the Labani Channel, and a 2,000-m-deep, 45-km-wide constriction as measured at the 50-m isobath (Smith & Sandwell, 1997; http://topex.ucsd.edu/marine_topo/) in Makassar Strait (Gordon et al., 1999). West of the deep Labani channel is a <10-m-deep coral reef rimming a broad promontory of generally <30 m deep, confining the throughflow to the Labani channel. The along-channel currents and transport estimates for Makassar Strait are based on the records from Aanderaa current meters on each mooring, set at depths of 200, 250, 350, and 750 m, with MAK-1 having a current meter at 1,500 m. Each mooring had an upward-looking Acoustic Doppler Current Profilers (ADCP) work horse set at 150 m.

2.2. INSTANT, January 2004 to Late November 2006

As part of an international program effort to simultaneously monitor the key ITF passageways, moorings were deployed in January 2004 near the Arlindo sites: $2^{\circ}51.9' \text{ S}$, $118^{\circ}27.3' \text{ E}$ (Mak-West) and $2^{\circ}51.5' \text{ S}$, $118^{\circ}37.7' \text{ E}$ (Mak-East), within Labani Channel (Gordon et al., 2008, 2010). The moorings were recovered and redeployed in July 2005, with final recovery on 27 November 2006. Both moorings were instrumented with upward-looking RD Instruments Long Ranger 75-kHz ADCP, at a nominal depth of 300 m. These were configured to measure all three velocity components in 10-m bins at 30-min intervals. A second 300-kHz ADCP was mounted looking down on both moorings, but data return from these instruments were poor, with a usable record only from the second deployment of Mak-East. Single point current meters were positioned on both moorings at 400 and 750 m. Additional current meters were positioned at 200 and 1,500 m on Mak-West.

2.3. MITF, November 2006 to August 2017 (Ongoing)

The Mak-West was redeployed as part of the MITF program upon recovery of the INSTANT moorings, on 22 November 2006. Mak-East was not redeployed. MITF was designed for data downloading and mooring rotation every 2 years. The only gap August 2011 to August 2013 was due to equipment shipping problems. The 2-year rotation was resumed in August 2013. The shallowest element in the November 2006 mooring, an upward-looking Long Ranger ADCP, was set at a depth of 463 m (at zero wire angle). A downward-looking Work Horse ADCP was set at 487 m. The two ADCP covered the Makassar throughflow to the 680-m sill depth (Gordon, Giulivi, & Ilahude, 2003). Aquadopp current meters were set at 475, 728, and 1,519 m. The 2009–2011 MITF mooring was similar in configuration to the 2007–2009, with slight depth changes as the mooring was set at a sea floor depth of ~20 m greater than that of the 2007–2009 mooring. The deployment occurred in April 2009, with recovery in August 2011. After the 2-year gap, the Mak-West mooring was deployed in August 2013 and recovered and redeployed in August 2015, placing both ADCP in the same buoy at 498 m and adding two χ -pods to measure temperature microstructure. The mooring was recovered in August 2017. Damage to the mooring during the August 2017 recovery delayed redeployment until 11 November 2017, using the configuration of the 2013–2015 mooring.

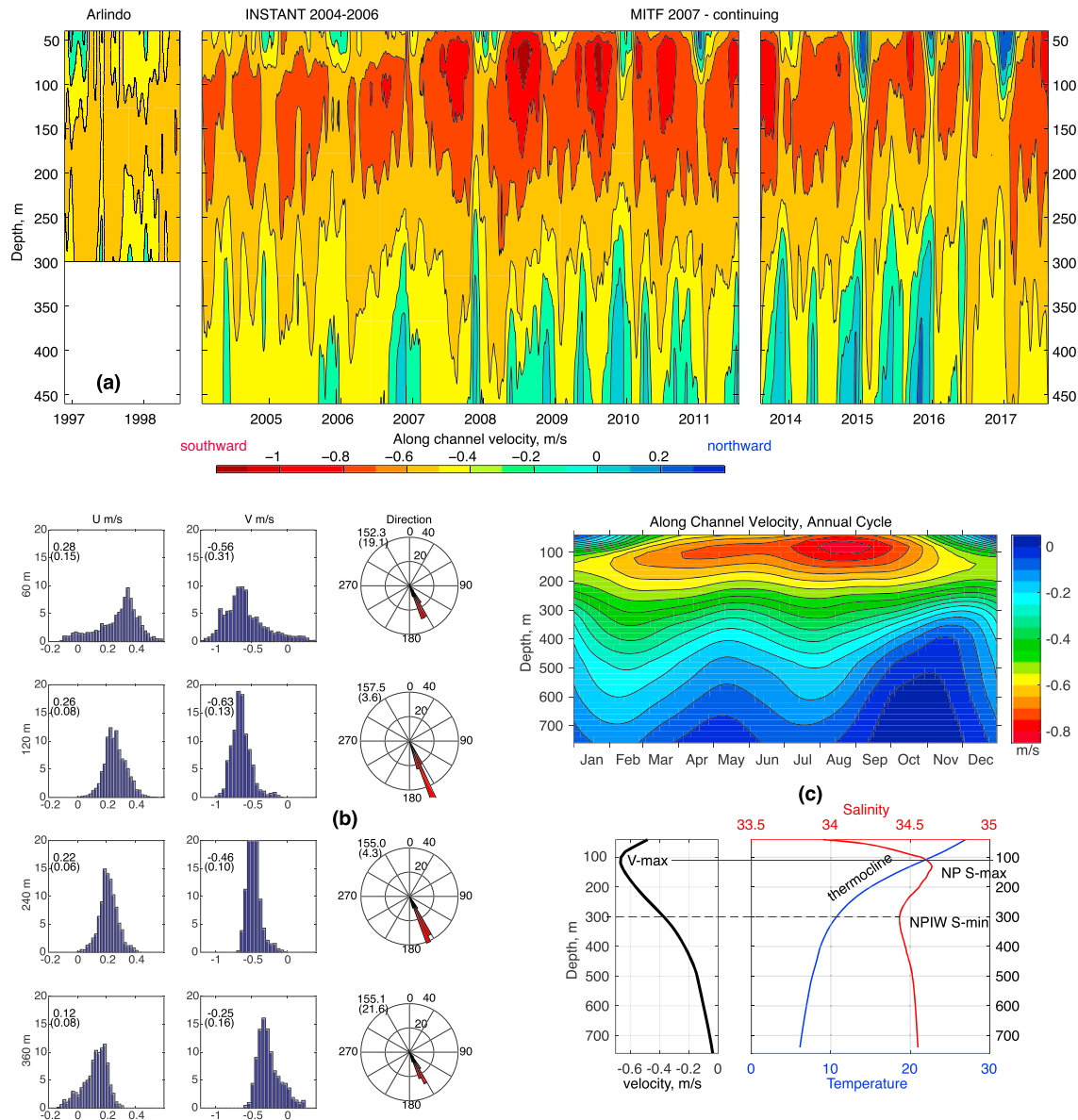


Figure 2. (a) Time series section 40 to 460 m from the Acoustic Doppler Current Profilers data, of the along-channel velocities (30-day running average; m/s) measured with Labani Channel. The average orientation of Labani Channel is 170° . The east-west and north-south (u and v) speeds were combined to yield the velocity along 170° . Negative values denote flow toward the south. (b) Histograms of U and V components of Makassar Strait Throughflow velocity in meters per second (left and center) and polar histogram of flow direction (right) at the depth level indicated to the left of the U/V histograms. Data shown are a 15-day running mean of hourly data, subsampled every 24 hr. Only measurements with a flow direction less than 300° are included, in order to exclude flow reversals in the near surface layer. For the U/V histograms, the mean and standard deviation (in parentheses) of velocity are given in the upper left of each histogram. For the direction polar histograms, then mean and standard deviation of direction are shown to the upper left of the polar plots. The vertical axes for U/V and radial axes on the polar histograms are percent. (c, upper panel) The annual cycle of along-channel speed (m/s). (lower panels) Mean annual along-channel velocity profile and temperature and salinity stratification for the 2004–2017 time series in Labani Channel (a). The temperature and salinity profiles were composed of CTD stations taken within Labani Channel during the Arlindo, INSTANT, and MITF programs. INSTANT = International Nusantara Stratification and Transport; MITF = Monitoring the Indonesian Throughflow; NPIW = North Pacific Intermediate Water.

2.4. Caveats

(1) The transport for the entire 13.3 years of time series (Figure 2a), is represented by the Mak-West mooring, as the Mak-East mooring was present only for 2004–2006. Following the Susanto et al. (2012) and Gordon et al. (2012) procedures, we use the Mak-West to represent the average Makassar Strait throughflow across the full width of Labani Channel. Of course, we would rather have had two (if not three mooring) to better

capture the Makassar Strait throughflow for the entire 13.3 years. Gordon et al. (2008) report that the INSTANT ratios of the Mak-East to Mak-West speeds average 0.95 (surface layer), 0.84 (midthermocline), and 0.76 (lower thermocline), which is consistent with the Arlindo observations (Gordon et al., 1999; Susanto & Gordon, 2005). The transport reported by Gordon et al. (2008) used an average of Mak-West and Mak-East velocity above 800 m. Using just the western site might lead to slightly higher transport but would not affect the transport variability since the Mak-West to Mak-East ratio does not vary significantly. (2) The average orientation of Labani Channel is 170° . The speed and transport values reported here are the flow directed along the 170° Labani Channel axis. Negative values denote flow toward the south. The mean directionality of the flow varies slightly with depth, albeit less than the Standard Deviation (Figure 2b) falling in the 152° to 158° slightly to eastward than the Labani Channel orientation, suggesting that the throughflow within Labani Channel must rotate southward as it transits through channel, as discussed by Metzger et al. (2010). To be consistent with previous studies, we present the speeds toward 170° . The difference in this speed to that of along 155° is minor, about 3–4% over all.

3. Data Views

3.1. Along-Channel Velocity Seasonal and Interannual Variability

Southward flow within Labani Channel of the Makassar Strait (Figure 2a) reaches a maximum during the boreal summer. Winter speeds are greatly reduced, often reaching zero or directed northward within the upper 100 m. The Makassar throughflow during 1997 was greatly diminished by an intense El Niño (Gordon et al., 1999), when sea level in the western tropical Pacific and associated Pacific to Indian Ocean pressure gradient was reduced (Clarke & Liu, 1994; Meyers, 1996; Wyrski, 1987). During the persistent La Niña conditions of 2008–2010, southward flow intensified as the sea level in the western tropical Pacific was higher relative to El Niño conditions (Hu et al., 2015; Sprintall et al., 2014).

The repeated Expendable Bathythermograph (XBT) section between Western Australia and Java (Feng et al., 2018; Liu et al., 2015; Wijffels et al., 2008) enables an upper-ocean geostrophic estimate of the ITF to be made extending back 30 years, with salinity estimated from climatological temperature-salinity relationships. The analysis of these data confirms that the ITF increases during La Niña and decreases during El Niño, but this effect is often weakened by in-phase wind forcing in the Indian Ocean associated with the Indian Ocean Dipole (IOD; Feng et al., 2018; Liu et al., 2015; Wijffels et al., 2008). The IOD is well coupled to ENSO but not always in-phase with ENSO (Cai et al., 2012; Chakravorty et al., 2014). Stuecker et al. (2017) find that about a third of IOD events occur independently of ENSO.

As the pathway from Makassar Strait to the IX1 line is not confined to an advective “pipe,” a direct comparison of the Makassar Strait throughflow transport to that crossing the IX1 line (Feng et al., 2018) is not straightforward. Most of the Makassar throughflow enters the Banda Sea, which has ~1-year residence time with strong vertical mixing before export into the Timor Sea of the eastern tropical Indian Ocean (Gordon et al., 2010). Additionally, the export from the Indonesian seas feeds into the South Equatorial Current and the Leeuwin Current pathways, which are likely not in-phase (Gruenburg & Gordon, 2018). Model studies (Song et al., 2004) find that it takes 2 to 3 years for the Makassar throughflow to reach the IX1 region. The increased Makassar southward flow in 2008 and 2009 (Figure 2a) may impact the IX1 transport in the 2010–2012 period. Perhaps the increased westward IX1 transport reported by Feng et al. (2018) in 2011 is a response to the Makassar Strait throughflow. Lee et al. (2015) report that cooling in the upper 700 m of the Pacific Ocean with commensurate heating of the Indian Ocean is linked to the increased ITF heat transport and may be related to the hiatus in global warming. The spreading of the ITF signal in the Indian Ocean is the topic for future research.

The southward velocity maximum (V -max) of nearly 0.7 m/s on average occurs within the 100- to 120-m depth interval of the upper thermocline (Figure 2a and lower two panels of Figure 2c), leading to a cooler ITF than if the V -max fell within the warm surface layer (Song & Gordon, 2004). The mean annual salinity profile (Figure 2c) reveals that the V -max falls within the salinity maximum core, marking North Pacific Subtropical Water (Gordon & Fine, 1996; Ilahude & Gordon, 1996). The velocity at 300 m near the salinity minimum core of the North Pacific Intermediate Water, at the 10°C isotherm, is about half of that at the V -max.

The southward flowing subsurface V-max within the Labani Channel (upper panel of Figure 2c) is most intense during in the boreal summer, July through September, with a mean speed of ~ 0.9 m/s, at a depth of ~ 70 m. There is a slow buildup to the summer V-max, spanning the 5-month period from February to July, from the weaker and deeper V-max of November–January. In contrast, the transition from the strong July–September V-max of summer to the weak V-max of November–January spans only 2 months, October into November, with the V-max core descending to near 150 m at ~ 0.5 m/s by December. The seasonality of the surface layer and V-max has been attributed to the winter injection of fresher, more buoyant surface layer water from the South China Sea and Java Sea into the southern Makassar Strait, which acts to inhibit southward pressure gradient and associated surface layer flow within Makassar Strait (the freshwater plug concept discussed by Gordon, Susanto, & Vranes, 2003; Gordon et al., 2012). The seasonal asymmetry of the freshwater plug buildup and decay may be a consequence the delayed injection of freshwater by river runoff from Kalimantan (Borneo).

From a larger-scale prospective, seasonal and interannual shifts in the latitude of the North Equatorial Current (NEC) Bifurcation along the east coast of The Philippines (Kim et al., 2004; Qiu & Chen, 2010; Qiu & Lukas, 1996; Qu & Lukas, 2003; Wang & Hu, 2006) affect the Makassar Strait transport profile (Gordon et al., 2012, 2014). When the NEC bifurcation is in a more northern position, as during the winter and during El Niño, the throughflow into the South China Sea via Luzon Strait is increased, enhancing the freshwater plug effect from the South China Sea, while the Mindanao Current strengthens, which reduces leakage into the Sulawesi Sea (and onto the Makassar Strait). Mindanao Current leakage increases as the NEC Bifurcation shifts southward, inducing a weaker Mindanao Current. The inverse relationship of the Mindanao Current strength and its leakage into the Sulawesi Sea is a product of the nonlinear inertia of the current, based on the retroreflection dynamics developed from the Agulhas retroreflection research (van Sebille et al., 2009). Thus, a more northern NEC Bifurcation (winter and El Niño) induces a deeper, weaker V-max in the Makassar throughflow. The opposite is true in the summer and during La Niña, when the NEC Bifurcation is in a more southern position.

It is noted that a lag exists between the Niño indices and the NEC Bifurcation latitude. Qiu and Chen (2010) find that the Niño3.4 leads the NEC bifurcation by 2 months; Qiu and Lukas (1996) find 5 months lead time. They also find the North Pacific wind stress curl leads the NEC bifurcation latitude: 6 months (Qiu & Chen, 2010) and 12 months (Qiu & Lukas, 1996). Qiu and Chen (2010) caution “the exact NEC bifurcation latitude depends on the surface wind forcing over the western tropical North Pacific Ocean containing variability not fully represented by the commonly used ENSO indices.” The same is no doubt also the situation for the Makassar Strait throughflow, and it is likely the lag relationship is a function of depth (Li et al.).

The heaving upward of the less than -0.1 -m/s isotach (Figure 2c, upper panel) during the April to June and the September to November periods is due to the penetration of strong downwelling Wyrтки Jet-related Kelvin Waves (WJKW), generated in the equatorial Indian Ocean during the monsoonal transition months (Reppin et al., 1999; Webster et al., 1999; Wyrтки, 1973), which enter Makassar Strait via Lombok Strait (Drushka et al., 2010; Pujiana et al., 2009, 2013; Shinoda et al., 2012; Sprintall et al., 2000).

Significant seasonal and interannual fluctuations are apparent (Figure 3a), with the depth of the V-max varying between 50 and 200 m, with the higher speeds scaling to the shallower depths at roughly 0.3 m/s/100 m and a root mean square of 0.10 m/s, reflecting the impact of interannual variability. Stronger, shallower V-max is characteristic of the summer and during La Niña periods. The strongest and shallowest V-max is recorded by the time series during La Niña periods, for example, 2008–2013 (except for a weak brief El Niño event in early 2010 transition months) when the injection of South China Sea low salinity surface layer water into the Makassar pathway is reduced (Gordon et al., 2012). A marked anomaly to this pattern is the deep, weak summer V-max of June and July 2016, falling well off the V-max/depth scatter (marked as a red star in Figure 3a). This event is induced by strong negative IOD, which increased sea level height in the eastern tropical Indian Ocean, reversing the Pacific to Indian Ocean pressure gradient facilitated substantial reduction of the upper-layer transport (this topic is covered in detail in Pujiana et al., 2019; revision in review).

The southward heat flux (HF; Figure 3b), relative to 0 °C, is a product of the along-channel current profiles determined by the Labani Channel time series and the temperature profiles, determined from the 2004–2006 mooring and ship-based Conductivity-Temperature-Depth recorder (CTD) profiles obtained during the

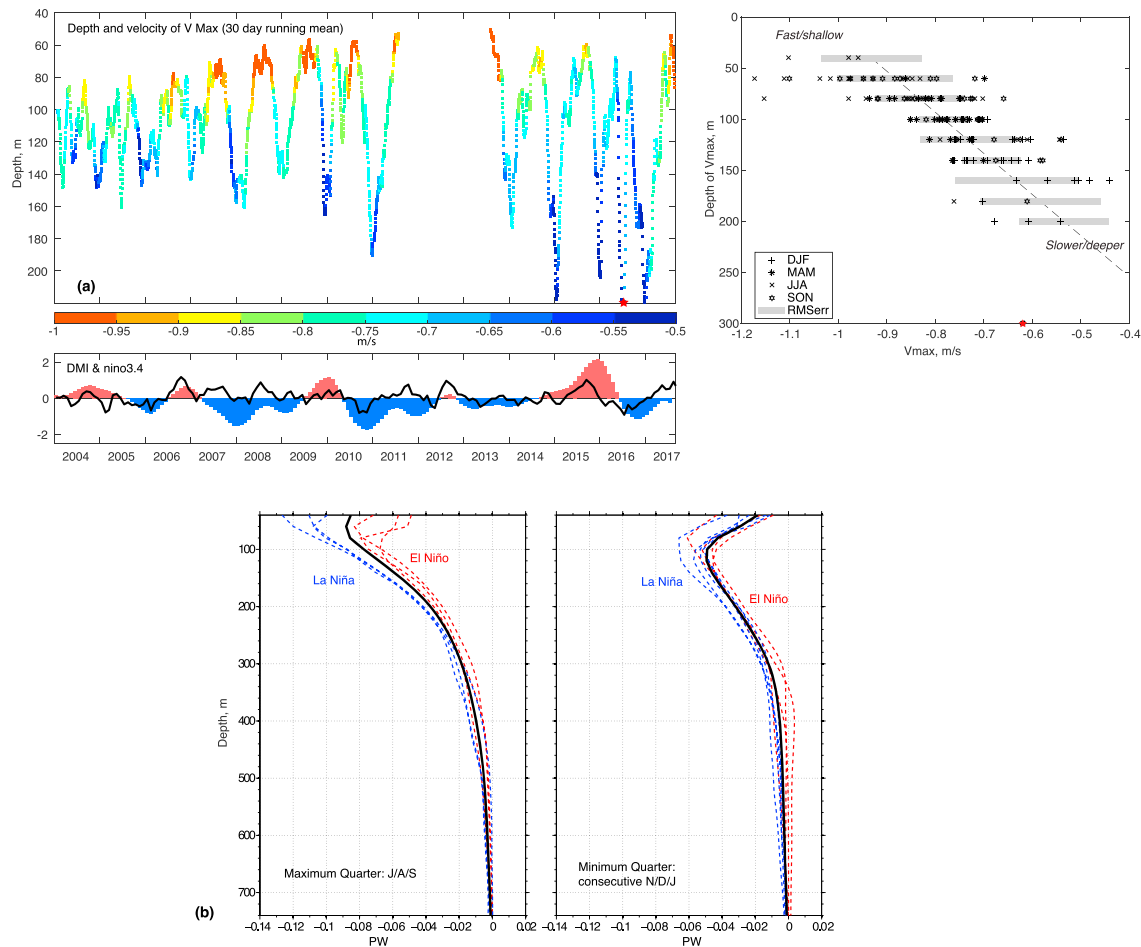


Figure 3. Figure 3 (a, upper left) Depth of the along-channel velocity maximum, color coded by velocity (m/s). The maximum velocities and corresponding grid bin (depth) were determined from the hourly data and then smoothed with a 30-day running average. The red star points to the anomalous June/July 2016 event. (lower left) The nino3.4 (red/blue bars; positive denoted El Niño; negative denoted La Niña) and DMI (Indian Ocean Dipole Mode Index; black line) time series. The indices were smoothed with a 6-month running mean. The smoothed index data were downloaded from Climate Explorer (<http://climexp.knmi.nl>). (right) Maximum along-channel speed versus depth of maximum speed. A 30-day block median filter was applied to the hourly data after computing the maximum for each hourly sample. The data are grouped according to season: DJF is December, January, February, and so forth. Time assigned to each block-median value is the median of the times of the hourly data comprising the block value. The dashed line represents the least-squares linear fit to all of the block median data, with an R^2 value of 0.50 and root mean square (RMS; gray bars) error of 0.10 m/s. (b) Makassar heat flux (HF) profile in PW/20 m (PW = Petawatt, 1015 Watts). The HF, relative to 0 °C, is a combination of along-channel velocity and temperature stratification. (left) HF profiles during the 3-month seasonal maximum southward HF July, August, and September (JAS). The thick black line denotes the mean JAS HF profile, blue dashed lines mark the JAS HF during La Niña (monthly nino3.4 less than or equal to -0.5) events of 2007, 2010, and 2011, and red dashed lines indicate JAS HF during El Niño (monthly nino3.4 greater than or equal to 0.5) events of 2004, 2006, and 2015. (right) HF profiles during the 3-month seasonal minimum southward HF November, December, and January (NDJ). The thick black line shows the mean NDJ HF profile, and the blue and red dashed lines display the NDJ HF during La Niña events of 2005–2006, 2007–2008, 2008–2009, 2010–2011, and 2016–2017 and NDJ HF during El Niño events of 2004–2005, 2009–2010, 2014–2015, and 2015–2016, respectively.

Arlindo, INSTANT, and MITF Labani Channel expeditions, combined with World Ocean Database CTD and XBT data within Makassar Strait since 1950. The boreal summer total HF of the 40- to 740-m water column ranges between -0.8 to -1.3 PW and in winter -0.1 to -0.5 PW. The average difference between the summer and winter southward HF is 0.7 PW (Gruenburg & Gordon, 2018). The southward HF peaks at shallower depths during the summer relative to winter. La Niña conditions are present during the maximum quarters of 2007, 2010, and 2011 and during the minimum quarters of 2005, 2007, 2008, 2010, and 2016. El Niño events occur during maximum quarters of 2004, 2006, and 2015 and minimum quarters of 2004/2005, 2009/2010, 2014/2015, and 2015/2016. ENSO impact on HF is most pronounced during the boreal summer, with the La Niña HF being much greater than the El Niño HF; the difference is reduced in the boreal winter (Figure 3b).

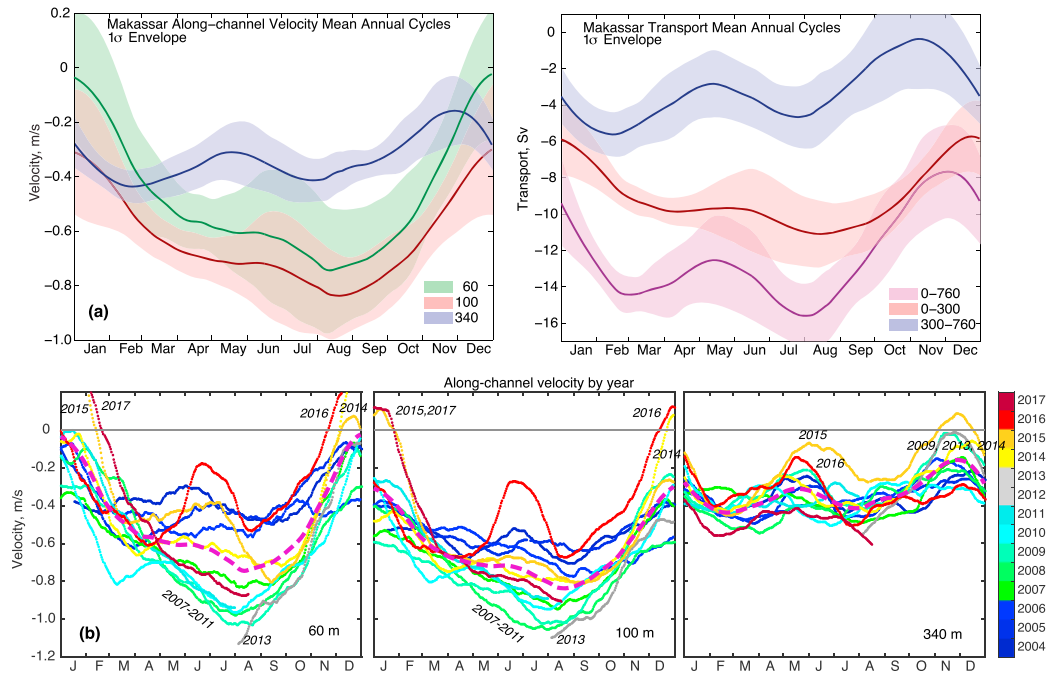


Figure 4. (a) Annual cycle of along-channel speed in the data grid bins indicated (left) and transport in the indicated levels (right). The color envelopes indicate one standard deviation about the mean. (b) Along-channel velocity for each year of recorded data, color coded by year, for the levels indicated. The data were filtered with a 60-day running mean, subsampled every 24 hr. The annual cycle of velocity is indicated as the dashed magenta line.

Gruenburg and Gordon (2018) report that following a rapid increase from 2006 to 2008, the southward Makassar HF Anomaly (HFa; relative to the average HF during the 2004–2017 observational period) peaks at 0.13 PW during 2008 and 2009. A subsequent slow decrease of Makassar HFa culminates in a -0.25 PW (less southward) minimum during 2015, followed by an increase. Gruenburg and Gordon (2018) find, at interannual time scales, that the vertical structure of the transport represented by the variability in the depth-dependent velocity profile is the major determinant of HFa, accounting for 78% of the variance in HFa, whereas changes in the temperature profile account for 28%. The total depth-integrated volume transport can explain only 57% of HFa variance as it does not reflect the relative contributions of the contrasting temperature of the depth slabs above and below 300 m (Figure 2b, lower left panel).

3.2. Annual Cycle and Anomalies of Velocity and Transport With Depth

The mean annual cycle of along-channel velocity and transport for three different depths (Figure 4a) brings out the depth dependence of the Makassar Strait throughflow. The summer maximum of southward flow is apparent at 100 m. The pattern of the velocities at 60 m is similar to that at 100 m but with speeds reduced by 0.1 to 0.2 m/s, reflecting the deeper subsurface V-max. At the 340-m base of the thermocline, a semiannual pattern is dominant, reflecting the intrusion of WJKW. The standard deviation in all three depths is largest in the winter and summer (the minimum and maximum throughflow occur), when the monsoonal winds are stronger, relative to the monsoonal transition seasons.

The 0- to 300-m transport (right panel of Figure 4a) is dominated by the annual cycle. A strong semiannual transport in the 300- to 760-m slab with reduced values in May and November reflects the influence of the WJKW. The highest correlation ($R = 0.76$) of the 0- to 300-m transport to that of the 300–760 m is found when upper layer lags deeper layer by 46 days. The lag may indicate an upward propagation on of the semi-annual WJKW with a phase speed of about 8 m/day, considerably slower than the speed attributed to an intraseasonal Kelvin wave discussed by Pujiana et al. (2013). A semiannual Kelvin wave vertically propagates at a slower phase speed than an intraseasonal Kelvin wave because the speed is inversely proportional to the wave period.

Viewing the annual cycle of along-channel velocity by year (Figure 4b) points to the features that contribute to the standard deviation (Figure 4a). The strongest southward flow (greater than -0.8 m/s) is observed in the summers of 2007–2011 and 2013 (note data gap August 2011 to July 2013) with increased southward flow in 2017. Relaxed or northward winter flows in the 60- and 100-m levels are most pronounced in the winters of 2014/2015 and 2016/2017. Seasonal variation and the MJO together account for the northward winter flow (Napitu, 2017). The MJO contributes to the northward flow by reversing the southward along-strait pressure gradient and increasing northward momentum transfer from wind stress. During the active phase of the MJO over the central Indonesian maritime continent, MJO westerly winds-driven Ekman transport increases sea surface height in the southern Makassar Strait, leading to a reduction in the southward along-strait pressure gradient (Napitu et al., this issue; in review). The suppressed southward along-strait pressure gradient and the northward component of the MJO winds, together, account for an increase in northward momentum transfer, contributing to the weakening of the southward flow in the upper 100 m during boreal winter (Napitu et al., 2019; in review).

Anomalous weakening of the southward throughflow occurred in the boreal summer of 2016 within the upper 300 m. Summer relaxation of the ITF in the upper 300-m layer as observed in 2016 is uncommon, as it is a condition characteristic of the winter season. The anomalous ITF relaxation during northern summer in 2016 may relate to the suppressed Pacific to Indian Ocean gradient in response to a significant negative IOD event (Figure 3a, lower panel; Pujiana et al., 2019; in revision), marked by higher than normal sea level in the eastern tropical Indian Ocean (Lim & Hendon, 2017; Lu et al., 2017). In June 2016, the ITF within the lower thermocline is composed of near zero or weak northward flow, substantially weaker than the mean annual cycle of the ITF in June of -0.3 m/s. A strong downwelling Kelvin wave within the Indian Ocean may have initiated the negative IOD event in 2016 (Lim & Hendon, 2017) and induced a strong relaxation in the ITF within Makassar Strait. The Indian Ocean downwelling Kelvin wave affects the ITF by increasing the sea surface height off the coasts of Java and Sumatra, reducing the interocean pressure gradient, and penetrating into Makassar Strait and thereby suppressing the southward ITF (Pujiana et al., 2019; in revision).

At 340 m, the weakest southward flow occurs in May–July and November–December, a marker of the WJKW intrusions (Pujiana et al., 2013; Sprintall et al., 2000). The most intense November–December WJKW influence occurred in 2009, 2013, 2014, and 2015, with the 2015 event being particularly strong, inducing northward flow. The 2015 May–June event was also the strongest in the Makassar throughflow time series. The May 2016 weakening was also large, but it was most pronounced in the June–July period in the 100-m level, as discussed above.

Interannual variation of the semiannual Kelvin wave in Makassar Strait reflects inter-annual variation of the Wyrki jet in the equatorial Indian Ocean. The strength of the equatorial jet varies with IOD, with negative IOD years exhibiting stronger jets (Duan et al., 2016; McPhaden et al., 2015). It appears that intensified Kelvin waves in Makassar Strait through the fall months of 2010, 2013, and 2014 coincide with negative IOD events.

3.3. Volume Transport

The 2004–2017 time series of the volume transport and their anomalies relative to the full time series mean, for upper 300 m and from 300 to 760 m (760 m which is 80 m deeper than the Makassar Strait topographic sill depth), plus the total Makassar throughflow, 0–760 m, are displayed in Figure 5. The mean temperature and standard deviation in the 0- to 300-m and 300- to 760-m intervals are 19.2 °C, 6.1 °C and 7.7 °C, 1.3 °C. The ratio of warm upper-layer transport to that of the cold lower layer (i.e. the velocity profile) is a major factor in the Makassar Strait HF (Gruenburg & Gordon, 2018). The 0- to 300-m transport layer, containing the North Pacific Subtropical Water (upper-thermocline S-max) and North Pacific Intermediate Water (S-min marking the base of the thermocline), represents the North Pacific surface and thermocline, injected into the ITF from the Mindanao Current (Gordon et al., 2012, 2014; Hu et al., 2015; Rudnick et al., 2015; Schönau et al., 2015). Below 300 m, Makassar Strait includes lower thermocline water and Antarctic Intermediate Water drawn from the South Pacific. South Pacific water masses are more dominant in the eastern passageways of the ITF (Ilahude & Gordon, 1996; Koch-Larrouy et al., 2008; Sprintall et al., 2014; Yang et al., 2018).

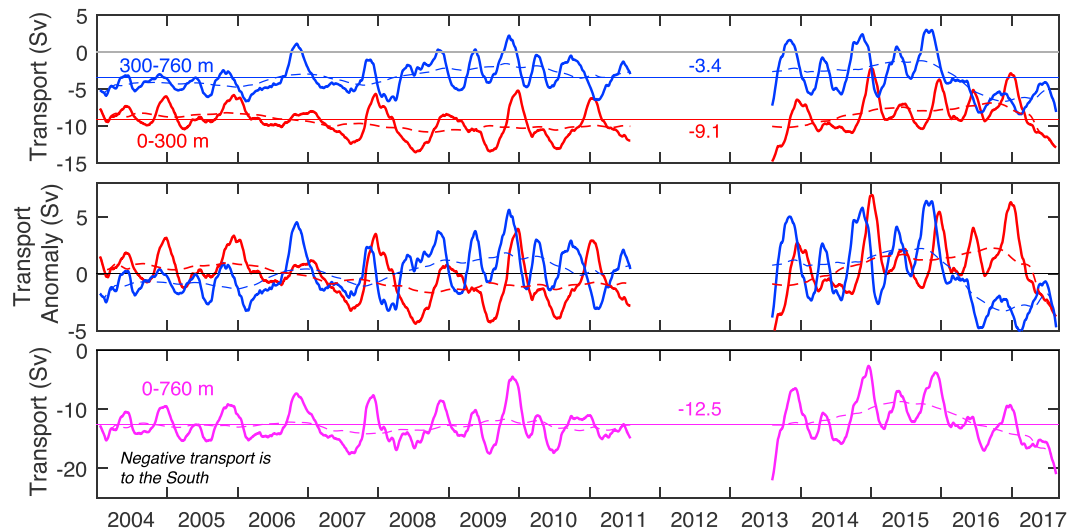


Figure 5. (upper panel) Volume transport in Sv (Sv, Sverdrup = $10^6 \text{ m}^3/\text{s}$) for the 0- to 300-m interval (red) and 300- to 760-m interval (blue). The 2004–2017 mean transports are indicated. For the calculation of the 0- to 300-m transport, the surface layer velocities (<40 m) were set to the uppermost observed value (Vranes et al., 2002). (middle panel) Transport anomaly from the 2004–2017 mean transport for the 0- to 300-m (red) and 300- to 760-m (blue) layers. (lower panel) Total transport 0–760 m. The 2004–2017 mean transport are indicated. The transports represent flow along the axis of Labani Channel, 350° to 170° orientation, subjected to a 60-day running mean and then subsampled at 24 hr. Negative values denote southward flow.

The 2004–2017 0- to 760-m transport average is 12.5 Sv; the 0- to 300-m average about 9.1 Sv; the 300- to 760-m transport is 3.4 Sv, a ratio of ~ 2.7 to 1. Thus, the upper 300 m supplies about 73% of the total Makassar throughflow or about 56% of the total ITF. During 2016, the ratio of the upper to the lower layers changed, reaching approximately 1:1 by mid-2016 (Figure 5). In 2017, with the return of La Niña, the 0–300 increases to >10 Sv, but 300- to 760-m transport remains high (Figure 5), driving the total transport to 20 Sv toward the end of the present time series in the summer of 2017.

4. Summary of Makassar Strait Throughflow, 2004–2017

The ITF transfers tropical Pacific Ocean water into the Indian Ocean, representing the only tropical interocean exchange pathway, and through air-sea forms an integral component of the climate system, specifically to ENSO and the Asian monsoon (Hu et al., 2015; Sprintall et al., 2014). The 13.3-year time series of the Makassar Strait throughflow, which carries $\sim 77\%$ of the total ITF (Gordon et al., 2010), reveals intraseasonal, seasonal, and interannual fluctuations, which reflect the regional- and larger-scale forcing within the Maritime Continent.

Consistent with earlier studies, which were based on a shorter Makassar Strait time series (Gordon et al., 2008, 2010; Susanto et al., 2012), the Makassar Strait throughflow exhibits strong southward transport during the boreal summer, relative to the winter (Figure 2). The seasonal signal is modulated by interannual ENSO forcing, with weaker southward flow and a deeper subsurface V-max during El Niño; stronger southward flow with a shallower V-max during La Niña (Figure 3). Interannual differences in the winter surface layer transport are associated with MJO passing over the Maritime Continent, with strong winter reversals occurring in 2014/2015 and 2016/2017 (Figure 2; Napitu et al., 2019). The strong weakening of the Makassar throughflow in observed in June 2016 (Figures 3a and 4b) can be attributed to a strong negative IOD (Pujiana et al., 2019).

The HF anomaly within Makassar Strait, a product of the along-channel current and temperature profiles, displays similar seasonal and interannual variability (Figure 3b; Gruenburg & Gordon, 2018). The annual cycle of the Makassar Strait throughflow velocity reveals changes with depth with significant interannual variability (Figures 3a and 4), responding to Kelvin Waves derived from the Indian Ocean with a distinct semiannual signal induced by the Wyrтки Jets (Figure 4; Pujiana et al., 2019).

During the entire time series, the average southward transport within the Makassar Strait (Figure 5) averaged 12.5 Sv, with the upper 300 m, composed of water imprinted with the North Pacific temperature/salinity, water mass, and characteristics (Figure 2c, lower panels), contributing 9.1 Sv (~73% of the total transport). The ratio of the transport between the upper 300-m slab and the transport within 300- to 760-m slab (noting the Makassar Strait sill depth is 680 m) averages 2.7 to 1 but exhibits seasonal and interannual fluctuations, attaining a 1:1 ratio in 2017. Interannual shifts in the ratio of the upper to lower layer transports are likely induced by the differences in the regions driving the transport, consistent with the depth-dependent water masses origins. The upper 300 m consisting of North Pacific water masses respond to the wind stress over the North Pacific (Li et al., 2018), whereas the lower slab composed of South Pacific water masses likely reflects factors from the greater realm. The southward transport within the Makassar Strait relaxed in 2014 and more so in 2015/2016 to less than 10 Sv (Figure 5), during a strong El Niño event (Figure 3a, lower panel), similar though not as extreme as during the strong El Niño event of 1997 (Gordon et al., 1999, 2008). Beginning in 2016 and extending into 2017 (the time series reported here extends only to August 2017), during a La Niña state, the Makassar Strait throughflow increased to ~20 Sv.

The fluctuations of the Makassar Strait throughflow reported here eventually spread across the Indian Ocean, affecting its heat and freshwater inventory. The Indian Ocean is likely just not a passive reactor to the Pacific forcing of the ITF but may feedback via to the Pacific (Yuan et al., 2011, 2013). Periods of La Niña increased ITF build up the heat inventory in the Indian Ocean (Lee et al., 2015). How does this feedback to the Pacific Ocean during a return to El Niño periods? This likely is related to the interplay between ENSO and the IOD, an active field of study (Sprintall & Révelard, 2014; van Sebille et al., 2014).

As the time series grows, it capture the decadal and longer period fluctuations, presently investigated with reanalysis and model products (Feng et al., 2018; Li et al., 2018; Tillinger & Gordon, 2009). Many of the Makassar Strait throughflow features reported here will be the subject for future detailed analysis, with model comparison, including the ITF transport profile, to the spatial and temporal patterns of the larger-scale ocean and climate systems.

Acknowledgments

Support provided by award UCAR Z15-17551 from the National Oceanic and Atmospheric Administration (NOAA), Division of Climate Observations, and U.S. Department of Commerce. This work was supported by NASA Headquarters under the NASA Earth and Space Science Fellowship Program—grant 80NSSC17K0438 Response of the Indian Ocean to Indonesian Throughflow Variability. The statements, findings, conclusions, and recommendations are those of the authors and do not necessarily reflect the views of NASA, NOAA, or the Department of Commerce. We appreciate important contributions of Ministry of Marine Affairs and Fisheries of the Republic of Indonesia for making arrangements to service the Makassar Strait mooring. K. P. was funded by National Research Council Research Associateship Award and performed this research at NOAA/PMEL. The Arlindo, INSTANT, and MITF Makassar data are available online (<https://www.ldeo.columbia.edu/~bhuber/MITF/>). Lamont-Doherty Earth Observatory contribution number 8283.

References

- Atmadipoera, A., Molcard, R., Madec, G., Wijffels, S., Sprintall, J., Koch-Larrouy, A., et al. (2009). Characteristics and variability of the Indonesian Throughflow water at the outflow straits. *Deep Sea Research*, 56(11), 1942–1954. <https://doi.org/10.1016/j.dsr.2009.06.004>
- Cai, W., van Rensch, P., Cowan, T., & Hendon, H. H. (2012). An asymmetry in the IOD and ENSO teleconnection pathway and its impact on Australian climate. *Journal of Climate*, 25(18), 6318–6329. <https://doi.org/10.1175/JCLI-D-11-00501.1>
- Chakravorty, S., Gnanaseelan, C., Chowdary, J. S., & Luo, J.-J. (2014). Relative role of El Niño and IOD forcing on the southern tropical Indian Ocean Rossby waves. *Journal of Geophysical Research: Oceans*, 119, 5105–5122. <https://doi.org/10.1002/2013JC009713>
- Clarke, A. J., & Liu, X. (1994). Interannual sea level in the Northern and Eastern Indian Ocean. *Journal of Physical Oceanography*, 24(6), 1224–1235. [https://doi.org/10.1175/1520-0485\(1994\)024<1224:ISLITN>2.0.CO;2](https://doi.org/10.1175/1520-0485(1994)024<1224:ISLITN>2.0.CO;2)
- Drushka, K., Sprintall, J., Gille, S. T., & Brodjonegoro, I. (2010). Vertical structure of Kelvin waves in the Indonesian Throughflow exit passages. *Journal of Physical Oceanography*, 40(9), 1965–1987. <https://doi.org/10.1175/2010JPO4380.1>
- Duan, Y., Liu, L., Han, G., Liu, H., Yu, W., Yang, G., et al. (2016). Anomalous behaviors of Wyrтки Jets in the equatorial Indian Ocean during 2013. *Scientific Reports*, 6(1), 29688. <https://doi.org/10.1038/srep29688>
- Feng, M., Zhang, N., Liu, Q., & Wijffels, S. (2018). The Indonesian throughflow, its variability and centennial change. *Geoscience Letters*, 5(3). <https://doi.org/10.1186/s40562-018-0102-2>
- Ffield, A., & Gordon, A. L. (1992). Vertical mixing in the Indonesian thermocline. *Journal of Physical Oceanography*, 22(2), 184–195.
- Ffield, A., & Gordon, A. L. (1996). Tidal mixing signatures in the Indonesian Seas. *Journal of Physical Oceanography*, 26(9), 1924–1937. [https://doi.org/10.1175/1520-0485\(1996\)026<1924:TMSITI>2.0.CO;2](https://doi.org/10.1175/1520-0485(1996)026<1924:TMSITI>2.0.CO;2)
- Ffield, A., Vranes, K., Gordon, A. L., Susanto, R. D., & Garzoli, S. L. (2000). Temperature variability within Makassar Strait. *Geophysical Research Letters*, 27(2), 237–240. <https://doi.org/10.1029/1999GL002377>
- Gordon, A. L., & Fine, R. (1996). Pathways of water between the Pacific and Indian oceans in the Indonesian seas. *Nature*, 379(6561), 146–149. <https://doi.org/10.1038/379146a0>
- Gordon, A. L., Flament, P., Villanoy, C., & Centurioni, L. (2014). The Nascent Kuroshio of Lamón Bay. *Journal of Geophysical Research: Oceans*, 119, 4251–4263. <https://doi.org/10.1002/2014JC009882>
- Gordon, A. L., Giulivi, C. F., & Ilahude, A. G. (2003). Deep topographic barriers within the Indonesian Seas. *Deep Sea Research Part II: Topical Studies in Oceanography*, 50, 2205–2228.
- Gordon, A. L., Huber, B. A., Metzger, E. J., Susanto, R. D., Hurlburt, H. E., & Adi, T. R. (2012). South China Sea Throughflow impact on the Indonesian Throughflow. *Geophysical Research Letters*, 39, L11602. <https://doi.org/10.1029/2012GL052021>
- Gordon, A. L., Sprintall, J., Van Aken, H. M., Susanto, D., Wijffels, S., Molcard, R., et al. (2010). The Indonesian Throughflow during 2004–2006 as observed by the INSTANT program. *Dynamics of Atmosphere and Oceans*, 50, 115–128.
- Gordon, A. L., Susanto, R. D., Ffield, A., Huber, B. A., Pranowo, W., & Wirasantosa, S. (2008). Makassar Strait Throughflow, 2004 to 2006. *Geophysical Research Letters*, 35, L24605. <https://doi.org/10.1029/2008GL036372>
- Gordon, A. L., Susanto, R. D., & Ffield, A. L. (1999). Throughflow within Makassar Strait. *Geophysical Research Letters*, 26(21), 3325–3328. <https://doi.org/10.1029/1999GL002340>

- Gordon, A. L., Susanto, R. D., & Vranes, K. (2003). Cool Indonesian throughflow is a consequence of restricted surface layer flow. *Nature*, 425(6960), 824–828. <https://doi.org/10.1038/nature02038>
- Gruenburg, L. K., & Gordon, A. L. (2018). Variability in Makassar Strait heat flux and its effect on the eastern tropical Indian Ocean. *Oceanography*, 31(2), 80–87. <https://doi.org/10.5670/oceanog.2018.220>
- Hautala, S. L., Sprintall, J., Potemra, J. T., Chong, J. C., Pandoe, W., Bray, N., & Ilahude, A. G. (2001). Velocity structure and transport of the Indonesian Throughflow in the major straits restricting flow into the Indian Ocean. *Journal of Geophysical Research*, 106(C9), 19,527–19,546. <https://doi.org/10.1029/2000JC000577>
- Hu, D., Wu, L., Cai, W., Gupta, A. S., Ganachaud, A., Qiu, B., et al. (2015). Pacific western boundary currents and their roles in climate. *Nature*, 522(7556), 299–308. <https://doi.org/10.1038/nature14504>
- Ilahude, A. G., & Gordon, A. L. (1996). Thermocline stratification within the Indonesian Seas. *Journal of Geophysical Research*, 101(C5), 12,401–12,409. <https://doi.org/10.1029/95JC03798>
- Kim, Y. Y., Qu, T., Jensen, T., Miyama, T., Mitsudera, H., Kang, H.-W., & Ishida, A. (2004). Seasonal and interannual variations of the North Equatorial Current bifurcation in a high resolution OGCM. *Journal of Geophysical Research*, 109, C03040. <https://doi.org/10.1029/2003JC002013>
- Koch-Larrouy, A., Lengaigne, M., Masson, S., Madec, G., & Terray, P. (2010). Indonesian tidal mixing effect on climate system. *Climate Dynamics*, 34(6), 891–904. <https://doi.org/10.1007/s00382-009-0642-4>
- Koch-Larrouy, A., Madec, G., Blanke, B., & Molcard, R. (2008). Quantification of the water paths and exchanges in the Indonesian archipelago. *Ocean Dynamics*. <https://doi.org/10.1007/s10236-008-0155-4>
- Koch-Larrouy, A., Madec, G., Bouruet-Aubertot, P., Gerkema, T., Bessieres, L., & Molcard, R. (2007). On the transformation of Pacific Water into Indonesian Throughflow Water by internal tidal mixing. *Geophysical Research Letters*, 34, L04604. <https://doi.org/10.1029/2006GL028405>
- Lee, S.-K., Park, W., Baringer, M. O., Gordon, A. L., Huber, B., & Liu, Y. (2015). Pacific origin of the abrupt increase in Indian Ocean heat content during the warming hiatus. *Nature Geoscience*, 8(6), 445–449. <https://doi.org/10.1038/ngeo2438>
- Li, M., Gordon, A. L., Wei, J., Gruenburg, L. K., & Jiang, G. (2018). Multi-decadal time series of the Indonesian Throughflow. *Dynamics of Atmospheres and Oceans*, 81, 84–95. <https://doi.org/10.1016/j.dynatmoce.2018.02.001>
- Lim, E.-P., & Hendon, H. (2017). Causes and predictability of the negative Indian Ocean Dipole and its impact on La Niña during 2016. *Scientific Reports*, 7(1), 12619. <https://doi.org/10.1038/s41598-017-12674-z>
- Liu, Q., Feng, M., Wang, D., & Wijffels, S. (2015). Interannual variability in the Indonesian Throughflow transport: A revisit based on 30 year expendable bathythermograph data. *Journal of Geophysical Research: Oceans*, 120, 8270–8282. <https://doi.org/10.1002/2015JC011351>
- Lu, B., Ren, H.-L., Scaife, A. A., Wu, J., Dunstone, N., Smith, D., et al. (2017). An extreme negative Indian Ocean Dipole event in 2016: Dynamics and predictability. *Climate Dynamics*, 1–12.
- McPhaden, M. J., Wang, Y., & Ravichandran, M. (2015). Volume transports of the Wyrtki jets and their relationship to the Indian Ocean Dipole. *Journal of Geophysical Research: Oceans*, 120, 5302–5317. <https://doi.org/10.1002/2015JC010901>
- Metzger, E. J., Hurlburt, H. E., Xu, X., Shriver, J. F., Gordon, A. L., Sprintall, J., et al. (2010). Simulated and observed circulation in the Indonesian Seas: 1/12° Global HYCOM and the INSTANT Observations. *Dynamics of Atmosphere and Oceans*, 50, 275–300.
- Meyers, G. (1996). Variation of Indonesian throughflow and El Niño - Southern Oscillation. *Journal of Geophysical Research*, 101(C5), 12,255–12,263. <https://doi.org/10.1029/95JC03729>
- Napitu, A. M. (2017). Response of the Indonesian Seas and its potential feedback to the Madden Julian Oscillation, PhD dissertation, Dept of Earth & Environmental Sciences, Columbia University. <https://doi.org/10.7916/D8086HSK>
- Napitu, A. M., Pujiana, K., & Gordon, A. L. (2019). The Madden-Julian Oscillation's Impact on the Makassar Strait Surface Layer Transport. *Journal of Geophysical Research: Oceans*, 124. <https://doi.org/10.1029/2018JC014729>
- Pujiana, K., Gordon, A. L., Metzger, E. J., & Field, A. L. (2012). The Makassar Strait pycnocline variability at 20–40 days. *Dynamics of Atmospheres and Oceans*, 53–54, 17–35.
- Pujiana, K., Gordon, A. L., & Sprintall, J. (2013). Intraseasonal Kelvin wave in Makassar Strait. *Journal of Geophysical Research: Oceans*, 118, 2023–2034. <https://doi.org/10.1002/jgrc.20069>
- Pujiana, K., Gordon, A. L., Sprintall, J., & Susanto, D. (2009). Intraseasonal variability in the Makassar Strait Thermocline. *Journal of Marine Research*, 67(6), 757–777. <https://doi.org/10.1357/002224009792006115>
- Pujiana, K., McPhaden, M. J., Gordon, A. L., & Napitu, A. M. (2019). Unprecedented response of Indonesian throughflow to anomalous Indo-Pacific climatic forcing in 2016. *Journal of Geophysical Research: Oceans*, 124. <https://doi.org/10.1029/2018JC014574>
- Qiu, B., & Chen, S. (2010). Interannual-to-decadal variability in the bifurcation of the North Equatorial Current off the Philippines. *Journal of Physical Oceanography*, 40(11), 2525–2538. <https://doi.org/10.1175/2010JPO4462.1>
- Qiu, B., & Lukas, R. (1996). Seasonal and interannual variability of the North Equatorial Current, the Mindanao Current and the Kuroshio along the Pacific western boundary. *Journal of Geophysical Research*, 101, 12,315–12,330.
- Qu, T., & Lukas, R. (2003). The bifurcation of the North Equatorial Current in the Pacific. *Journal of Physical Oceanography*, 33(1), 5–18. [https://doi.org/10.1175/1520-0485\(2003\)033<0005:TBOTNE>2.0.CO;2](https://doi.org/10.1175/1520-0485(2003)033<0005:TBOTNE>2.0.CO;2)
- Reppin, J., Schott, F. A., Fischer, J., & Quadfasel, D. (1999). Equatorial currents and transports in the upper central Indian Ocean: Annual cycle and interannual variability. *Journal of Geophysical Research*, 104(C7), 15,495–15,514. <https://doi.org/10.1029/1999JC900093>
- Rudnick, D. L., Jan, S., & Lee, C. M. (2015). A new look at circulation in the western North Pacific. *Oceanography*, 28(4), 16–23. <https://doi.org/10.5670/oceanog.2015.77>
- Schönau, M. C., Rudnick, D. L., Cerovecki, I., Gopalakrishnan, G., Cornuelle, B. D., McClean, J. L., & Qiu, B. (2015). The Mindanao Current: Mean structure and connectivity. *Oceanography*, 28(4), 34–45. <https://doi.org/10.5670/oceanog.2015.79>
- Shinoda, T., Han, W., Jensen, T., Zamudio, L., Metzger, E. J., & Lien, R.-C. (2016). Impact of the Madden-Julian Oscillation on the Indonesian Throughflow in the Makassar Strait during the CINDY/DYNAMO Field Campaign. *Journal of Climate*, 29(17), 6085–6108. <https://doi.org/10.1175/JCLI-D-15-0711.1>
- Shinoda, T., Han, W., Metzger, E. J., & Hurlburt, H. E. (2012). Seasonal variation of the Indonesian Throughflow in Makassar Strait. *Journal of Physical Oceanography*, 42(7), 1099–1123. <https://doi.org/10.1175/JPO-D-11-0120.1>
- Smith, W., & Sandwell, D. (1997). Global sea floor topography from satellite altimetry and ship depth soundings. *Science*, 277(5334), 1956–1962. <https://doi.org/10.1126/science.277.5334.1956>
- Song, Q., & Gordon, A. (2004). Significance of the vertical profile of Indonesian Throughflow transport on the Indian Ocean. *Geophysical Research Letters*, 31, L16307. <https://doi.org/10.1029/2004GL020360>
- Song, Q., Gordon, A. L., & Visbeck, M. (2004). Spreading of the Indonesian Throughflow in the Indian Ocean. *Journal of Physical Oceanography*, 34(4), 772–792. [https://doi.org/10.1175/1520-0485\(2004\)034<0772:SOTITI>2.0.CO;2](https://doi.org/10.1175/1520-0485(2004)034<0772:SOTITI>2.0.CO;2)

- Sprintall, J., Gordon, A., Murtugudde, R., & Susanto, D. (2000). A semi-annual Indian Ocean forced Kelvin wave observed in the Indonesian Seas in May 1997. *Journal of Geophysical Research*, *105*(C7), 17,217–17,230. <https://doi.org/10.1029/2000JC900065>
- Sprintall, J., Gordon, A. L., Koch-Larrouy, A., Lee, T., Potemra, J. T., Pujiana, K., & Wijffels, S. E. (2014). The Indonesian Seas and their impact on the Coupled Ocean Climate System. *Nature Geoscience*, *7*, 487–492. <https://doi.org/10.1038/NGEO2188>
- Sprintall, J., & Révelard, A. (2014). The Indonesian Throughflow response to Indo-Pacific climate variability. *Journal of Geophysical Research: Oceans*, *119*, 1161–1175. <https://doi.org/10.1002/2013JC009533>
- Stuecker, M. F., Timmermann, A., Jin, F.-F., Chikamoto, Y., Zhang, W., Wittenberg, A. T., et al. (2017). Revisiting ENSO/Indian Ocean Dipole phase relationships. *Geophysical Research Letters*, *44*, 2481–2492. <https://doi.org/10.1002/2016GL072308>
- Susanto, R. D., Ffield, A., Gordon, A. L., & Adi, T. R. (2012). Variability of Indonesian Throughflow within Makassar Strait: 2004 – 2009. *Journal of Geophysical Research*, *117*, C09013. <https://doi.org/10.1029/2012JC008096>
- Susanto, R. D., & Gordon, A. L. (2005). Velocity and transport of Indonesian Throughflow in Makassar Strait. *Journal of Geophysical Research*, *110*, C01005. <https://doi.org/10.1029/2004JC002425>
- Tillinger, D., & Gordon, A. L. (2009). Fifty years of the Indonesian Throughflow. *Journal of Climate*, *22*(23), 6342–6355. <https://doi.org/10.1175/2009JCLI2981.1>
- van Sebille, E., Biastoch, A., van Leeuwen, P. J., & de Ruijter, W. P. M. (2009). A weaker Agulhas Current leads to more Agulhas leakage. *Geophysical Research Letters*, *36*, L03601. <https://doi.org/10.1029/2008GL036614>
- van Sebille, E., Sprintall, J., Schwarzkopf, F. U., Gupta, A. S., Santoso, A., England, M. H., et al. (2014). Pacific-to-Indian Ocean connectivity: Tasman leakage, Indonesian Throughflow, and the role of ENSO. *Journal of Geophysical Research: Oceans*, *119*, 1365–1382. <https://doi.org/10.1002/2013JC009525>
- Vranes, K., Gordon, A. L., & Ffield, A. (2002). The heat transport of the Indonesian throughflow and implications for the Indian Ocean Heat Budget. *Deep-Sea Research*, *49*(7,8), 1391–1410.
- Wajsowicz, R. C., Gordon, A. L., Ffield, A., & Susanto, R. D. (2003). Estimating transport in Makassar Strait. *Deep Sea Research, Part II*, *50*, 2163–2181.
- Wang, Q., & Hu, D. (2006). Bifurcation of the North Equatorial Current derived from altimetry in the Pacific Ocean. *Journal of Hydrodynamics*, *18*(5), 620–626. [https://doi.org/10.1016/S1001-6058\(06\)60144-3](https://doi.org/10.1016/S1001-6058(06)60144-3)
- Webster, P. J., Moore, A. M., Loschnigg, J. P., & Leben, R. R. (1999). Coupled ocean–atmosphere dynamics in the Indian Ocean during 1997–98. *Nature*, *401*(6751), 356.
- Wijffels, S. E., Meyers, G. M., & Godfrey, J. S. (2008). A 20-year average of the Indonesian Throughflow: Regional currents and the inter-basin exchange. *Journal of Physical Oceanography*, *38*(9), 1965–1978. <https://doi.org/10.1175/2008JPO3987.1>
- Wyrtki, K. (1973). An equatorial jet in the Indian Ocean. *Science*, *181*(4096), 262–264. <https://doi.org/10.1126/science.181.4096.262>
- Wyrtki, K. (1987). Indonesian Throughflow and the associated pressure gradient. *Journal of Geophysical Research*, *92*(C12), 12,941–12,946. <https://doi.org/10.1029/JC092iC12p12941>
- Yang, L., Zhou, L., Li, S., & Wei, Z. (2018). Spreading of the South Pacific Tropical Water and Antarctic Intermediate Water Over the Maritime Continent. *Journal of Geophysical Research: Oceans*, *123*, 4423–4446. <https://doi.org/10.1029/2018JC013831>
- Yuan, D., Wang, J., Xu, T., Xu, P., Hui, Z., Zhao, X., et al. (2011). Forcing of the Indian Ocean dipole on the interannual variations of the tropical Pacific Ocean: Roles of the Indonesian throughflow. *Journal of Climate*, *24*(14), 3593–3608. <https://doi.org/10.1175/2011JCLI3649.1>
- Yuan, D., Zhou, H., & Zhao, X. (2013). Interannual climate variability over the tropical Pacific Ocean induced by the Indian Ocean dipole through the Indonesian Throughflow. *Journal of Climate*, *26*(9), 2845–2861. <https://doi.org/10.1175/JCLI-D-12-00117.1>